Dalton Transactions

Rocksalt-type heavy rare earth monoxides TbO, DyO, and ErO exhibiting the metallic electronic states and ferromagnetism

Journal:	*Dalton Transactions*
Manuscript ID	DT-ART-11-2024-003214
Article Type:	Paper
Date Submitted by the Author:	16-Nov-2024

Complete List of Authors:	Sasaki, Satoshi; Tohoku University, Oka, Daichi; Tokyo Metropolitan University, Department of Chemistry; Tohoku University - Aobayama Campus Shiga, Daisuke; Tohoku University, Multidisciplinary Research for Advanced Materials Takahashi, Ryunosuke; University of Hyogo School of Science Graduate School of Material Science Nakata, Suguru; University of Hyogo School of Science Graduate School of Material Science Harata, Koichi; Tohoku University Institute for Materials Research Yamasaki, Yuichi; National Institute for Materials Science Kitamura, Miho; National Institutes for Quantum Science and Technology Nakao, Hironori; Photon Factory, Institute of Materials Structure Science, High Energy Accelerator Research Organization, Wadati, Hiroki; University of Hyogo School of Science Graduate School of Material Science Kumigashira, Hiroshi; High Energy Accelerator Research Organisation, Photon Factory, Institute of Materials Structure Science; Tohoku University, Institute of Multidisciplinary Research for Advanced Materials Fukumura, Tomoteru; Tohoku University, Department of Chemistry; Tohoku University, WPI-Advanced Institute for Materials Research

ARTICLE

Rocksalt-type heavy rare earth monoxides TbO, DyO, and ErO exhibiting the metallic electronic states and ferromagnetism †

Received 00th January 20xx,
Accepted 00th January 20xx

DOI: 10.1039/x0xx00000x

Satoshi Sasaki[a], Daichi Oka[a,b], Daisuke Shiga[c], Ryunosuke Takahashi[d], Suguru Nakata[d], Koichi Harata[e], Yuichi Yamasaki[f], Miho Kitamura[g,h], Hironori Nakao[g], Hiroki Wadati[d], Hiroshi Kumigashira[c,g] and Tomoteru Fukumura*[a,i,j]

Solid-phase rare earth monoxides have been recently synthesized via thin film epitaxy. However, it has been difficult to synthesize heavy rare earth monoxides owing to the severe chemical instability. In this study, rocksalt-type heavy rare earth monoxides *RE*Os (*RE* = Tb, Dy, Er) were synthesized for the first time, as single-phase epitaxial thin films. The *RE*Os were characterized by hard X-ray photoemission spectroscopy, X-ray absorption spectroscopy, resonant photoemission spectroscopy, and magnetization measurements. These *RE*Os showed the metallic electronic states with the almost localized 4f states, indicating the $4f^n5d^1$ electronic configurations of Tb, Dy, and Er ions. X-ray magnetic circular dichroism measurements of TbO evidenced the magnetic ordering of the 4f spins below the Curie temperature (T_C). The T_C was evaluated to be 233 K for TbO, 142 K for DyO, and 88 K for ErO, where the T_C decreased with the 4f electron's number, approximately proportional to the de Gennes factor.

Introduction

Chemically stable binary rare earth oxides are usually rare earth sesquioxides RE_2O_3 with the RE^{3+} ions (*RE* = Sc, Y, lanthanoids), which are highly insulating and dielectric.[1] In contrast, rare earth monoxides *RE*Os are metastable phases.[2] Among them, only EuO and YbO have been frequently studied because of their chemical stability of the Eu^{2+} and Yb^{2+} ions owing to the half or fully filled 4f orbitals.[1] Since EuO is an archetypal ferromagnetic semiconductor with the Curie temperature (T_C) of 69 K,[3] other *RE*Os with partially filled 4f orbitals are expected to exhibit intriguing electronic and magnetic properties. In the 1980s, light *RE*Os (LaO, CeO, PrO, NdO, and SmO) were synthesized as the metallic bulk polycrystals by high-pressure synthesis,[2] which were considered to be contaminated with the rare earth metal.[4] Recently, single-phase light *RE*Os (LaO, CeO, PrO, NdO, and SmO) were successfully synthesized via thin film epitaxy.[5–9] LaO is a superconductor,[5] CeO is a paramagnetic metal,[6] PrO and NdO are low-T_C (28 and 19 K, respectively) ferromagnetic metals,[7,8] and SmO is a paramagnetic metal.[9] Similarly, heavy *RE*Os (GdO, TbO, HoO, and LuO) were synthesized as the epitaxial thin films.[10–13] GdO, TbO, and HoO showed much higher T_C than the light *RE*Os (276, 231, and 131 K, respectively),[10–12] except for paramagnetic LuO with fully filled 4f orbitals of Lu^{2+} ion.[13] Those heavy *RE* ions with partially filled 4f orbitals possess large total angular momenta due to the parallel coupling of spin and unquenched orbital angular momenta as was seen in heavy *RE* nitrides *RE*Ns,[14] in addition to the much higher T_C of the heavy *RE*Os than those of the *RE*Ns. Such high T_C, strong magnetization, and large spin-orbit interaction would be attractive for magnetics and spintronics. However, a sizable amount of RE_2O_3 phase contained in most of the heavy *RE*O thin films obscured their intrinsic physical properties, e.g., the poor electrical conduction in GdO and TbO despite the presence of 5d electron carriers.[10,11] Also, DyO and ErO are expected to be high T_C ferromagnets, but have not been synthesized yet except for the minor byproducts in RE_2O_3 synthesized under high vacuum.[15,16] Thus, single-phase heavy *RE*Os have been strongly desired to unveil their intrinsic physical properties and to elucidate the origin of their high T_C.

In the previous studies on the light *RE*O thin films, the thin film epitaxy was effective to stabilize the metastable *RE*Os on suitable lattice-matched single crystal substrates. However, the heavier *RE*Os possess smaller lattice constants due to the lanthanoid contraction, which enhanced the lattice mismatch between *RE*O thin films and commercial substrates. Previously, rocksalt-type SrO buffer layer was used to obtain highly

[a] Department of Chemistry, Graduate School of Science, Tohoku University, Sendai 980-8578, Japan Email: tomoteru.fukumura.e4@tohoku.ac.jp
[b] Department of Chemistry, Graduate School of Science, Tokyo Metropolitan University, Tokyo 192-0397, Japan
[c] Institute of Multidisciplinary Research for Advanced Materials, Tohoku University, Sendai 980-8577, Japan
[d] Graduate School of Material Science, University of Hyogo, Hyogo 678-1297, Japan
[e] Institute for Materials Research, Tohoku University, Sendai 980-8577, Japan
[f] Center for Basic Research on Materials, National Institute for Materials Science (NIMS), Tsukuba, Ibaraki 305-0047, Japan
[g] Photon Factory, Institute of Materials Structure Science, High Energy Accelerator Research Organization (KEK), Tsukuba 305-0801, Japan
[h] NanoTerasu Center, National Institutes for Quantum Science and Technology (QST), Sendai, Miyagi 980-8572, Japan
[i] WPI Advanced Institute for Materials Research, Tohoku University, Sendai 980-8577, Japan
[j] Center for Science and Innovation in Spintronics, Organization for Advanced Studies, Tohoku University, Sendai 980-8577, Japan
† Electronic Supplementary Information available. See DOI: 10.1039/x0xx00000x

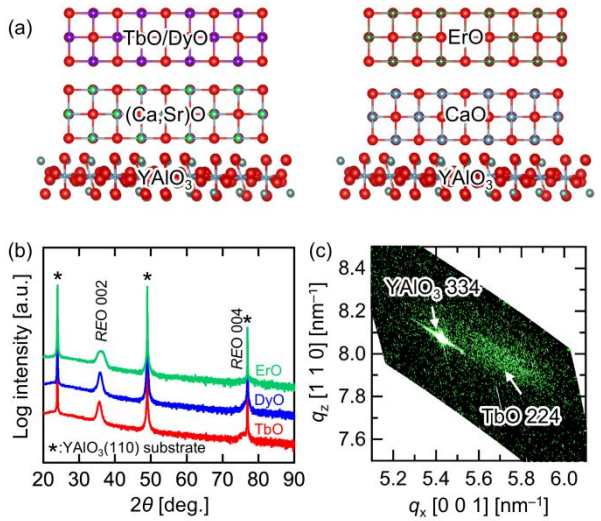

Fig. 1 (a) Schematic crystal structure of TbO or DyO thin films on (Ca,Sr)O buffer layer (left) and ErO thin film on CaO buffer layer (right) on $YAlO_3$ substrate. (b) XRD ϑ–2ϑ patterns for the TbO, DyO, and ErO thin films on the buffer layers. (c) Reciprocal space map around the TbO 224 diffraction and the $YAlO_3$ 334 diffraction peaks for the TbO thin film.

crystalline EuO (lattice constant: 5.16 Å) epitaxial thin film,[17–19] although the SrO (5.14 Å) layer cannot be applied universally to other *RE*Os whose lattice constants are broadly distributed: from LaO (5.295 Å)[5] to YbO (4.87 Å) .[20] And recently, rocksalt-type CaO buffer layer was used to improve the crystallinity of the GdO thin film.[21] In this study, we developed a rocksalt-type (Ca,Sr)O solid-solution buffer layer, whose lattice constant is tunable by the composition, being suitable for thin film growth of the various heavy *RE*Os (Fig. 1a), where the lattice mismatches between the thin film and the buffer layer for TbO and DyO except for ErO were significantly reduced in comparison with those between the thin film and $YAlO_3$ substrate (Table 1). As a result, single-phase TbO, DyO, and ErO were synthesized for the first time as the epitaxial thin films. Contrary to the preliminary result of nonpure-phase TbO that was reported to be semiconducting,[11] these compounds possessed metallic electronic states, being consistent with the $4f^n5d^1$ electronic configuration. In addition, DyO and ErO were discovered to be ferromagnetic. Their T_C was systematically changed with respect to the f-electron number: T_C = 233 K (TbO), 142 K (DyO), and 88 K (ErO).

Table 1 Lattice constants of *RE*O thin films, $YAlO_3$ substrate, and buffer layers with their lattice mismatches.

*RE*O	Substrate/ buffer layer	Mismatch [%]
TbO	$YAlO_3$(×√2)	–4.24
c = 5.03 Å	5.26 Å	
a = 4.90 Å	$(Ca_{0.5}Sr_{0.5})O$	–0.20
V = 120.8 Å^3	5.04 Å	
DyO	$YAlO_3$(×√2)	–4.82
c = 5.00 Å	5.26 Å	
a = 4.88 Å	$(Ca_{0.5}Sr_{0.5})O$	–0.79
V = 119.8 Å^3	5.04 Å	
ErO	$YAlO_3$(×√2)	–5.39
c = 4.97 Å	5.26 Å	
a = 4.84 Å	CaO	4.41
V = 116.4 Å^3	4.76 Å	

Experimental

Thin film growth

TbO, DyO, and ErO epitaxial thin films were grown by pulsed laser deposition with a KrF excimer laser (λ = 248 nm). $(Ca_{0.5}Sr_{0.5})O$ buffer layer was used for the TbO and DyO thin films, and CaO buffer layer was used for the ErO thin film. Prior to deposition, $YAlO_3$ (110) single crystal substrate was preannealed at 1200 °C for 4 hours to have a step-and-terrace surface.[5] The buffer layers were grown on the substrates at 600−700 °C under 5.0 × 10^{-6} Torr of oxygen, where $(Ca_{0.5}Sr_{0.5})CO_3$ polycrystalline target was sintered with spark plasma sintering (Fig. S1†) and CaO (99.9%) polycrystalline target were used for the $(Ca_{0.5}Sr_{0.5})O$ and CaO buffer layers, respectively. Subsequently, the *RE*O thin films were grown on the buffer layers at 150 °C under 5 × 10^{-8} Torr of oxygen, where Tb, Dy, and Er metal (99.9%) targets were used for the corresponding *RE*O thin films. The detailed growth conditions are summarized in Table 2. To prevent the film oxidation, 2−5 nm-thick amorphous AlO_x capping layers were *in-situ* deposited on the thin films at room temperature. During deposition, film growth was monitored by *in-situ* reflection high-energy electron diffraction (RHEED).

Structure analysis

The crystal structure was evaluated by X-ray diffraction with Cu

Table 2 Deposition parameters of buffer layers, *RE*O thin films, and capping layer.

Layer	Target	T_{sub} [°C]	P_{O2} [Torr]	E_{laser} [J/cm^2]	Frequency [Hz]	Thickness [nm]
$(Ca_{0.5}Sr_{0.5})O$	$(Ca_{0.5}Sr_{0.5})CO_3$	700	5.0×10^{-6}	0.50	10	5
CaO	CaO	600	5.0×10^{-6}	0.50	20	10
TbO	Tb	150	5.0×10^{-8}	0.70	10	10
DyO	Dy	150	5.0×10^{-8}	0.60	10	10
ErO	Er	150	5.0×10^{-8}	0.60	10	10
AlO_x	Al_2O_3	R.T.	–	0.70	10	5

*T_{sub}: substrate temperature; P_{O2}: oxygen pressure during growth; E_{laser}: energy density of laser spot.

$K\alpha_1$ radiation (XRD, D8 Discover, Bruker AXS and SmartLab, Rigaku).

Synchrotron X-ray spectroscopy

For the electronic states, hard X-ray photoemission spectroscopy (HAXPES) was performed by using a Scienta R-4000 electron energy analyzer with a total energy resolution of 200 meV at a photon energy of 8 keV at BL09XU of SPring-8. Also, X-ray absorption spectroscopy (XAS) and *RE* 3d-4f resonant photoemission spectroscopy (RPES) were performed with total electron yield mode at BL-2A MUSASHI of Photon Factory, KEK. The RPES spectra were recorded at various photon energies *hv* around the Tb, Dy, and Er 3d-4f thresholds for resonant photoemission measurement, where *hv*s of on- and off-resonances were determined by measuring XAS at the Tb, Dy, and Er M_5 absorption edges. The Fermi level (E_F) was calibrated by the measurement of a gold film that was electrically connected to the *RE*O thin films. X-ray magnetic circular dichroism (XMCD) spectroscopy was performed with total electron yield mode to measure Tb M_4 and M_5 absorption edges at BL-16A of the Photon Factory, KEK.

Magnetization measurements

The magnetization was measured by a superconducting quantum interference device magnetometer (MPMS-3, Quantum Design). The thin films were mounted to the straw holders. The diamagnetic signals from the holder and substrate were corrected by subtracting the magnetic-field-linear component of the magnetization fitted at high magnetic field.

Results and discussion

Fig. 1b shows XRD θ–2θ patterns of the TbO, DyO, and ErO thin films on $YAlO_3$ substrates with the buffer layers (Table 1). The *RE*O 002 and 004 diffraction peaks overlapped with the (Ca,Sr)O 00*l* or CaO 00*l* diffraction peaks (Fig. S2†) were observed without any impurity phases. Out-of-plane lattice constants of the thin films were $c = 5.03$ Å (TbO), 5.00 Å (DyO), and 4.97 Å (ErO). Since the lattice mismatch of the ErO thin film was not significantly reduced by using the buffer layer (Table 1), not only the small lattice mismatch but also the rocksalt-type buffer layer was appropriate for the epitaxial stabilization of the *RE*O thin films. The spot 224 peak of the TbO thin film in reciprocal space mapping (Fig. 1c) confirmed the epitaxial relationship of TbO [001] || $YAlO_3$ [110] and TbO [110] || $YAlO_3$ [001]. Epitaxial growth of the DyO (001) and ErO (001) thin films was also confirmed by reciprocal space mapping, *in-situ* RHHED patterns, and φ scan measurements (Fig. S3–S5†, respectively) with the same epitaxial relationship. The lattice mismatch between the thin film and the buffer layer was larger in the order of TbO, DyO, and ErO thin films, resulting in the less crystallinity, as seen in the broader XRD peak intensity, the broader RHEED streak patterns, and asymmetric peaks of the phi scan for DyO and ErO thin films (Fig. 1, Fig. S3−S5†). The obtained lattice constants are summarized in Table 1. The ionic radii of the 6-coordinated RE^{2+} ions were 1.07 Å (Tb^{2+}), 1.06 Å (Dy^{2+}), and 1.04 Å (Er^{2+}), evaluated from the cube root of the cell volumes. These values were approximately the same as ionic radii of the RE^{2+} ions calculated from the Shannon's ionic radii of 6-coordinated RE^{2+} ions: 1.10 Å (Tb^{2+}), 1.09 Å (Dy^{2+}), and 1.06 Å (Er^{2+}).[22]

Fig. 2 shows the HAXPES spectra of the TbO, DyO, and ErO thin films at room temperature. The *RE* 3d core level peaks shifted monotonically with the atomic numbers (Fig. 2a). The Tb and Dy peaks located between those of *RE* metal and RE_2O_3 (Table S1†),[23–25] indicating the ionic character of TbO and DyO (the formal ionic charge of Tb^{2+} and Dy^{2+} ions in TbO and DyO, respectively), while HAXPES 3d core level spectra of Er and Er_2O_3 have not been not reported. The valence band spectra of *RE*O thin films showed the *RE* 5d states distributed within 4 eV below E_F and the existence of Fermi edges (Fig. 2b), similar to CeO, PrO, and SmO epitaxial thin films,[6,7,27] while the O 2p state and *RE* 4f multiplet[28] of the *RE*Os for 6–10 eV were probably overlapped with the O 2p states and Al 3s states due to the comparable photoionization cross section of *RE* 4f and Al 3s.[29] This result indicates that the TbO, DyO, and ErO epitaxial thin films possessed the metallic electronic states, where the 5d electrons formed the conduction band near E_F.

Fig. 3a−c show XAS spectra for the TbO, DyO, and ErO thin films taken at *RE* M_4 and M_5 edges together with the theoretical spectra calculated for the RE^{3+} states.[30] The good agreement of XAS spectra between the *RE*O, the theoretical calculations, and *RE* metals[30] indicates that an outer electron configuration of *RE* ions was $4f^n5d^16s^2$ [the 4f electron number of *RE* ion in *RE*O was $4f^n$ (n = 8, 9, and 11 for Tb^{2+}, Dy^{2+}, and Er^{2+}, respectively)]. From the HAXPES results in Fig. 2, the presence of $5d^1$-electron-derived conduction band at E_F was confirmed. Accordingly, the electronic configuration of the *RE* ion side in *RE*O is $4f^85d^1$ (TbO), $4f^95d^1$ (DyO), and $4f^{11}5d^1$ (ErO), while the $6s^2$ electrons are accommodated in the O 2p−*RE* 6s bonding states. Fig. 3d−i show *RE* 3d-4f RPES spectra taken at corresponding photon energies for on- and off-resonances at the M_5 absorption edges. Owing to the giant resonance enhancement for the 4f states, the 4f derived states were extracted irrespective of the presence of the AlO_x capping layer. At E_F, intensity for the on-resonance states was insignificantly enhanced in comparison with those of CeO and PrO,[6,7] representing a small 4f contribution to the states

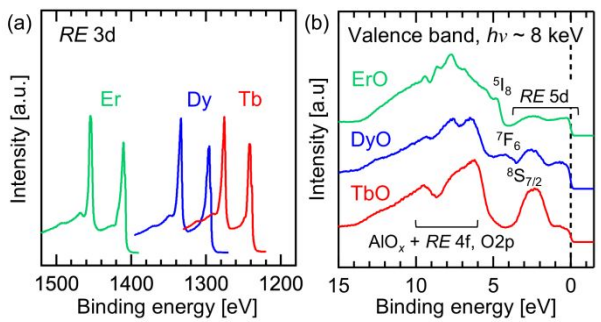

Fig. 2 HAXPES spectra of the TbO, DyO, and ErO thin films. (a) The *RE* 3d core level spectra and (b) the valence band spectra. The observed spectra between 6–10 eV are attributed to O 2p and *RE* 4f multiplet of the *RE*Os, probably overlapped with that of amorphous AlO_x capping layer, whose band gap was reported to be ~3.64 eV.[26]

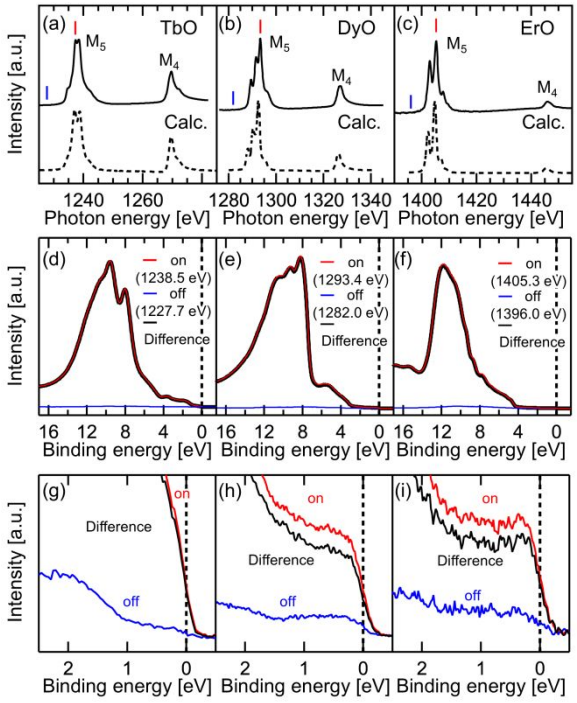

Fig. 3 XAS spectra for (a) TbO, (b) DyO, and (c) ErO thin films around the *RE* M_4 and M_5 edges (solid line) together with the calculated spectra (dashed line) for the RE^{3+} states. Valence band RPES spectra for (d, g) TbO, (e, h) DyO, and (f, i) ErO thin films with (g–i) the magnified data around E_F.

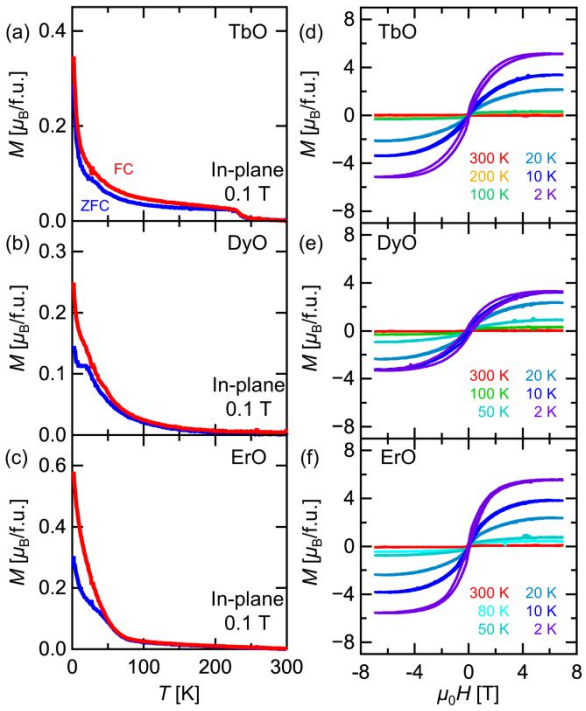

Fig. 4 (a–c) Temperature dependence of magnetization for (a) TbO, (b) DyO, and (c) ErO thin films under field-cooling (FC) and zero-field-cooling (ZFC). Magnetic field of 0.1 T was applied along in-plane. (d–f) Magnetic field dependence of magnetization for (d) TbO, (e) DyO, and (f) ErO thin films at different temperatures. Magnetic field was applied along in-plane.

near E_F. Meanwhile, the 4f-derived multiplet structures around 8 eV for TbO, at 8 eV for DyO, and at 12 eV for ErO were strongly enhanced for on-resonant spectra. These results indicate that the majority of 4f electrons are localized so that the hybridization between conduction and f electrons is weak in TbO, DyO, and ErO in contrast with CeO and PrO.[6,7]

Fig. 4a–c show the temperature dependence of magnetization for the *RE*O thin films under field-cooling (FC) and zero-field-cooling (ZFC). Since the onsets of magnetization were not clearly observed for DyO and ErO (Fig. 4b,c) , the T_C of DyO and ErO were evaluated from the onsets of $dM/dT-T$ curves, whereas the T_C of TbO was evaluated from the negative peak of $dM/dT-T$ curve (Fig. S6†) like that of EuO,[31] where the evaluated T_C was consistent with $M^{-1}-T$ curves (Fig. S6†). The evaluated T_C was 233 K (TbO), 142 K (DyO), and 88 K (ErO). It is noted that the T_C was lower for the heavier *RE*Os similar to rocksalt-type rare earth nitrides *RE*Ns,[32] in spite of their significantly lower T_C: T_C = 42 K (TbN), 26 K (DyN), and 5 K (ErN). Fig. 4d–f show the magnetic field dependence of magnetization for the *RE*O thin films at different temperatures. The magnetic hysteresis loops were observed up to 200 K, 100 K, and 80 K for TbO, DyO, and ErO, respectively, being consistent with the T_C described above and the temperature dependence of the coercive force (Fig. S6†). The saturation magnetization at 2 K and 7 T was 5.1 μ_B/f.u. (TbO), 3.2 μ_B/f.u. (DyO), and 5.6 μ_B/f.u. (ErO). These values were smaller than the theoretical magnetic moments of the trivalent rare earth ions [9 μ_B (Tb^{3+}), 10 μ_B (Dy^{3+}), and 9 μ_B (Er^{3+})]. The smaller magnetic moments have often been observed for rare earth nitrides,[33,34] possibly attributed to crystal field effects,[32,35] noncollinear spin structure,[36] and/or antiferromagnetic superexchange coupling between *RE*–O–*RE* bonds. The smaller magnetization of DyO among them could be caused by the larger lattice mismatch (Table 1) as well as large anisotropy of 4f orbital.[37] In Fig. 4d, the wasp-waisted hysteresis was not observed in TbO in contrast with the previous study,[11] probably because the Tb_2O_3 impurity phase in the previous study served as a pinning center of the magnetic domain wall motion resulting in the wasp-waisted hysteresis.[38]

Fig. 5 shows XAS and XMCD spectra around Tb M_5 and M_4 absorption edges of the TbO thin film at 9 K and 1.25 T. The XAS spectrum of the TbO thin film was consistent with that in Fig. 3a. The TbO thin film clearly showed nonzero intensity in XMCD spectrum, whose multiplet feature corresponded to that of the XAS spectrum. The multiplet feature, despite the different spectral shape, was similar to that of $Tb_3Fe_5O_{12}$ garnet [39] rather than that of Tb based alloy.[40] These results reflect the ferromagnetic states of the RE^{3+} ions in *RE*Os. The XMCD M_5 peak monotonically decreased with increasing temperature up to 100 K (inset of Fig. 5). Accordingly, the 4f and 5d global ferromagnetic order was formed below the T_C contrary to the previous study's suggestion that the 4f and 5d ferromagnetic sublattices form below 20 K and T_C, respectively.[11]

The much higher T_C of TbO, DyO, and ErO than those of TbN (42 K), DyN (26 K), and ErN (5 K) would be attributed to a principal role of the 5d conducting carriers for Ruderman-Kittel-Kasuya-Yosida (RKKY) interaction, taking into account the $4f^n5d^1$ and $4f^n5d^0$ electronic configurations of the *RE*Os and

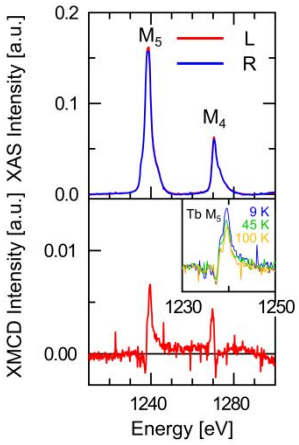

Fig. 5 XAS and corresponding XMCD spectra at 9 K of the TbO thin film. Inset shows temperature dependence of Tb M_5 peak in XMCD spectrum. Magnetic field of 1.25 T was applied along out-of-plane.

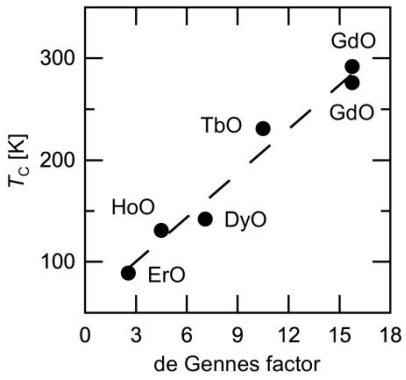

Fig. 6 Curie temperatures of heavy rare earth monoxides as a function of the de Gennes factor $\xi = (g-1)^2 J(J+1)$, where g is the Lande's g-factor and J is the total angular momentum quantum number. The T_C of HoO and GdO are cited from previous studies.[10,12,21]

*RE*Ns, respectively. This is why the T_C of *RE*Ns is enhanced by increasing carrier concentration through N deficiency.[41,42] The T_C of *RE*Os decreased with increasing 4f electron's number similar to heavy rare earth metals.[43] The T_C of heavy rare earth alloys is a monotonically increasing function of the de-Gennes factor ξ,[44] well scaled by $\xi^{2/3}$.[45] In contrast, the T_C of heavy *RE*Os was rather proportional to ξ (Fig. 6), although this origin is unclear at present. It is also noted that the oxygen content in *RE*O could influence their electronic states and magnetism, since GdO was found to show significant dependence of electric and magnetic properties on the oxygen content.[10,21] Further investigation on this matter is necessary, although the precise control of the oxygen content in *RE*O is also challenging.

Conclusion

Rocksalt-type heavy rare earth monoxides TbO, DyO, and ErO were synthesized as the single phase epitaxial thin films by utilizing epitaxial force from lattice-matching-tunable buffer layer. These rare earth ions possessed [Xe]$4f^n5d^1$ electronic configurations, and 4f and 5d electrons served as localized and conduction electrons, respectively, indicating the metallic electronic states even above Curie temperature in contrast with the semiconducting EuO.[3] Much higher Curie temperatures of TbO, DyO, and ErO than those of corresponding heavy rare earth mononitrides suggest significant influence of RKKY interaction owing to the 5d conduction electrons.

Author contributions

S. Sasaki: Investigation, Methodology, Data curation, Funding acquisition, Writing-original draft, Writing-review & editing. D. Oka: Investigation, Data curation, Funding acquisition, Writing-original draft, Writing-review & editing. D. Shiga: Investigation, Data curation, Funding acquisition, Writing-original draft, Writing-review & editing. R. Takahashi: Investigation, Data curation, Writing-review & editing. S. Nakata: Investigation, Data curation, Writing-original draft, Writing-review & editing. K. Harata: Investigation, Data curation, Writing-review & editing. Y. Yamasaki: Resources, Data curation, Funding acquisition, Writing-review & editing. M. Kitamura: Resources, Data curation, Writing-review & editing. H. Nakao: Resources, Data curation, Writing-review & editing. H. Wadati: Resources, Funding acquisition, Data curation, Writing-original draft, Writing-review & editing. H. Kumigashira: Resources, Funding acquisition, Data curation, Writing-original draft, Writing-review & editing. T. Fukumura: Resources, Supervision, Data curation, Funding acquisition, Writing-original draft, Writing-review & editing. All authors read and approved the final manuscript.

Conflicts of interest

There are no conflicts to declare.

Acknowledgements

The authors thank Cooperative Research and Development Center for Advanced Materials, Tohoku University for technical assistance, and Dr. Kenta Amemiya for technical supports of XMCD measurements. The HAXPES experiment at SPring-8 was conducted with approval from the Japan Synchrotron Radiation Research Institute (Proposal No. 2022B1574). The work performed at KEK-PF was approved by the Program Advisory Committee (Proposals No. 2022G675, No. 2021S2-002, and No. 2021S2-004) at the Institute of Materials Structure Science, KEK. S.S was supported by Grant-in-Aid of Tohoku University, Division for Interdisciplinary Advanced Research and Education. This work was in part supported by JSPS-KAKENHI (Grant No. 20H02704, 21H05008) and JST SPRING (Grant No. JPMJSP2114).

References

1 G. Y. Adachi and N. Imanaka, The Binary Rare Earth Oxides, *Chem. Rev.*, 1998, **98**, 1479–1514.

2 J. M. Leger, N. Yacoubi and J. Loriers, Synthesis of Rare Earth Monoxides, *J. Solid State Chem.*, 1981, **36**, 261–270.

3 A. Mauger and C. Godart, The Magnetic, Optical, and Transport Properties of Representatives of a Class of Magnetic Semiconductors: The Europium Chalcogenides, *Phys. Rep.*, 1986, **141**, 51–176.

4 L. R. Morss and R. J. M. Konings, in *Binary Rare Earth Oxides*, Springer Netherlands, Dordrecht, 2004, pp. 163–188.

5 K. Kaminaga, D. Oka, T. Hasegawa and T. Fukumura, Superconductivity of Rock-Salt Structure LaO Epitaxial Thin Film, *J. Am. Chem. Soc.*, 2018, **140**, 6754–6757.

6 N. Abe, D. Oka, K. Kaminaga, D. Shiga, D. Saito, T. Yamamoto, N. Kimura, H. Kumigashira and T. Fukumura, Rocksalt CeO Epitaxial Thin Film as a Heavy-Fermion System Transiting from *p*-Type Metal to Partially Compensated *n*-Type Metal by 4*f* Delocalization, *Phys. Rev. B*, 2022, **106**, 125106.

7 H. Shimizu, D. Oka, K. Kaminaga, D. Saito, T. Yamamoto, N. Abe, N. Kimura, D. Shiga, H. Kumigashira and T. Fukumura, Rocksalt-Type PrO Epitaxial Thin Film as a Weak Ferromagnetic Kondo Lattice, *Phys. Rev. B*, 2022, **105**, 014442.

8 D. Saito, K. Kaminaga, D. Oka and T. Fukumura, Itinerant Ferromagnetism in Rocksalt NdO Epitaxial Thin Films, *Phys. Rev. Mater.*, 2019, **3**, 064007.

9 Y. Uchida, K. Kaminaga, T. Fukumura and T. Hasegawa, Samarium Monoxide Epitaxial Thin Film as a Possible Heavy-Fermion Compound, *Phys. Rev. B*, 2017, **95**, 125111.

10 T. Yamamoto, K. Kaminaga, D. Saito, D. Oka and T. Fukumura, Rock Salt Structure GdO Epitaxial Thin Film with a High Ferromagnetic Curie Temperature, *Appl. Phys. Lett.*, 2020, **117**, 052402.

11 S. Sasaki, D. Oka, K. Kaminaga, D. Saito, T. Yamamoto, N. Abe, H. Shimizu and T. Fukumura, A High-T_C Heavy Rare Earth Monoxide Semiconductor TbO with a More than Half-Filled 4f Orbital, *Dalt. Trans.*, 2022, **51**, 16648–16652.

12 T. Amrillah, D. Oka, H. Shimizu, S. Sasaki, D. Saito, K. Kaminaga and T. Fukumura, Rock Salt-Type HoO Epitaxial Thin Film as a Heavy Rare-Earth Monoxide Ferromagnetic Semiconductor with a Curie Temperature above 130 K, *Appl. Phys. Lett.*, 2022, **120**, 082403.

13 K. Kaminaga, D. Oka, T. Hasegawa and T. Fukumura, New Lutetium Oxide: Electrically Conducting Rock-Salt LuO Epitaxial Thin Film, *ACS Omega*, 2018, **3**, 12501–12504.

14 F. Natali, B. J. Ruck, N. O. V. Plank, H. J. Trodahl, S. Granville, C. Meyer and W. R. L. Lambrecht, Rare-Earth Mononitrides, *Prog. Mater. Sci.*, 2013, **58**, 1316–1360.

15 V. K. Kaul and O. N. Srivastava, On the Existence of Dysprosium Monoxide Phase, *Japanese J. Appl. Physics, Part 1 Regul. Pap. Short Notes Rev. Pap.*, 1976, **15**, 1801–1802.

16 U. Saxena and O. N. Srivastava, Unusual Thickness Dependence of the Dielectric Constant of Erbium Oxide Films, *Thin Solid Films*, 1976, **33**, 185–192.

17 H. Miyazaki, H. Momiyama, T. Hajiri, T. Ito, K. Imura, M. Matsunami and S. Kimura, Fabrication of Single Crystalline EuO Thin Film with SrO Buffer Layer on $SrTiO_3$ Substrate, *J. Phys. Conf. Ser.*, 2012, **391**, 012047.

18 J. Lettieri, V. Vaithyanathan, S. K. Eah, J. Stephens, V. Sih, D. D. Awschalom, J. Levy and D. G. Schlom, Epitaxial Growth and Magnetic Properties of EuO on (001) Si by Molecular-Beam Epitaxy, *Appl. Phys. Lett.*, 2003, **83**, 975–977.

19 R. Held, J. A. Mundy, M. E. Holtz, D. Hodash, T. Mairoser, D. A. Muller and D. G. Schlom, Fabrication of Chemically and Structurally Abrupt $Eu_{1-x}La_xO$/SrO/Si Interfaces and Their Analysis by STEM-EELS, *Phys. Rev. Mater.*, 2021, **5**, 124419.

20 T. Yamamoto, K. Kaminaga, D. Saito, D. Oka and T. Fukumura, High Electron Mobility with Significant Spin-Orbit Coupling in Rock-Salt YbO Epitaxial Thin Film, *Appl. Phys. Lett.*, 2019, **114**, 162104.

21 T. Fukasawa, D. Kutsuzawa, D. Oka, K. Kaminaga, D. Saito, H. Shimizu, H. Naganuma and T. Fukumura, Enhanced Curie Temperature near 300 K in Highly Crystalline GdO Epitaxial Thin Films Concomitant with an Anomalous Hall Effect, *J. Mater. Chem. C*, 2024, **12**, 7652–7657.

22 Y. Q. Jia, Crystal Radii and Effective Ionic Radii of the Rare Earth Ions, *J. Solid State Chem.*, 1991, **95**, 184–187.

23 B. D. Padalia, W. C. Lang, P. R. Norris, L. M. Watson and D. J. Fabian, X-Ray Photoelectron Core-Level Studies of the Heavy Rare-Earth Metals and Their Oxides, *Proc. R. Soc. London. A. Math. Phys. Sci.*, 1977, **354**, 269–290.

24 D. J. Morgan, Core-Level Spectra of Metallic Lanthanides: Dysprosium (Dy), *Surf. Sci. Spectra*, 2023, **30**, 024017.

25 D. Barreca, A. Gasparotto, A. Milanov, E. Tondello, A. Devi and R. A. Fischer, Nanostructured Dy_2O_3 Films: An XPS Investigation, *Surf. Sci. Spectra*, 2007, **14**, 52–59.

26 E. O. Filatova and A. S. Konashuk, Interpretation of the Changing the Band Gap of Al_2O_3 Depending on Its Crystalline Form: Connection with Different Local Symmetries, *J. Phys. Chem. C*, 2015, **119**, 20755–20761.

27 S. Sakamoto, K. Kaminaga, D. Oka, R. Yukawa, M. Horio, Y. Yokoyama, K. Yamamoto, K. Takubo, Y. Nonaka, K. Koshiishi, M. Kobayashi, A. Tanaka, A. Yasui, E. Ikenaga, H. Wadati, H. Kumigashira, T. Fukumura and A. Fujimori, Hard and Soft X-Ray Photoemission Spectroscopy Study of the New Kondo System SmO Thin Film, *Phys. Rev. Mater.*, 2020, **4**, 095001.

28 J. K. Lang, Y. Baer and P. A. Cox, Study of the 4f and Valence Band Density of States in Rare-Earth Metals. I. Theory of the 4f States, *J. Phys. F Met. Phys.*, 1981, **11**, 121–138.

29 J. J. Yeh and I. Lindau, Atomic Subshell Photoionization Cross Sections and Asymmetry Parameters: $1 \leqslant Z \leqslant 103$, *At. Data Nucl. Data Tables*, 1985, **32**, 1–155.

30 B. T. Thole, G. van der Laan, J. C. Fuggle, G. A. Sawatzky, R. C. Karnatak and J. M. Esteva, 3d X-Ray-Absorption Lines and the $3d^9\,4f^{n+1}$ Multiplets of the Lanthanides, *Phys. Rev. B*, 1985, **32**, 5107–5118.

31 H. Miyazaki, H. J. Im, K. Terashima, S. Yagi, M. Kato, K. Soda, T. Ito and S. Kimura, La-Doped EuO: A Rare Earth Ferromagnetic Semiconductor with the Highest Curie Temperature, *Appl. Phys. Lett.*, 2010, **96**, 232503.

32 H. R. Child, Neutron Diffraction Investigation of the Magnetic Properties of Compounds of Rare-Earth Metals with Group V Anions, *Phys. Rev.*, 1963, **131**, 922–931.

33 J. P. Evans, G. A. Stewart, J. M. Cadogan, W. D. Hutchison, E. E. Mitchell and J. E. Downes, Magnetic Structure of DyN: A ^{161}Dy Mössbauer Study, *Phys. Rev. B*, 2017, **95**, 054431.

34 E.-M. Anton, J. F. McNulty, B. J. Ruck, M. Suzuki, M. Mizumaki, V. N. Antonov, J. W. Quilty, N. Strickland and H. J. Trodahl, NdN: An Intrinsic Ferromagnetic Semiconductor, *Phys. Rev. B*, 2016, **93**, 064431.
35 G. T. Trammell, Magnetic Ordering Properties of Rare-Earth Ions in Strong Cubic Crystal Fields, *Phys. Rev.*, 1963, **131**, 932–948.
36 C. Meyer, B. J. Ruck, A. R. H. Preston, S. Granville, G. V. M. Williams and H. J. Trodahl, Magnetic Properties of ErN Films, *J. Magn. Magn. Mater.*, 2010, **322**, 1973–1978.
37 S.-D. Jiang and S.-X. Qin, Prediction of the Quantized Axis of Rare-Earth Ions: The Electrostatic Model with Displaced Point Charges, *Inorg. Chem. Front.*, 2015, **2**, 613–619.
38 Q. Gao, G. Hong, J. Ni, W. Wang, J. Tang and J. He, Uniaxial Anisotropy and Novel Magnetic Behaviors of $CoFe_2O_4$ Nanoparticles Prepared in a Magnetic Field, *J. Appl. Phys.*, 2009, **105**, 07A516.
39 E. Rosenberg, J. Bauer, E. Cho, A. Kumar, J. Pelliciari, C. A. Occhialini, S. Ning, A. Kaczmarek, R. Rosenberg, J. W. Freeland, Y. Chen, J. Wang, J. LeBeau, R. Comin, F. M. F. de Groot and C. A. Ross, Revealing Site Occupancy in a Complex Oxide: Terbium Iron Garnet, *Small*, 2023, **19**, 2300824.
40 D. H. Suzuki, M. Valvidares, P. Gargiani, M. Huang, A. E. Kossak and G. S. D. Beach, Thickness and Composition Effects on Atomic Moments and Magnetic Compensation Point in Rare-Earth Transition-Metal Thin Films, *Phys. Rev. B*, 2023, **107**, 134430.
41 N. O. V. Plank, F. Natali, J. Galipaud, J. H. Richter, M. Simpson, H. J. Trodahl and B. J. Ruck, Enhanced Curie Temperature in N-Deficient GdN, *Appl. Phys. Lett.*, 2011, **98**, 112503.
42 W. F. Holmes-Hewett, C. Pot, R. G. Buckley, A. Koo, B. J. Ruck, F. Natali, A. Shaib, J. D. Miller and H. J. Trodahl, Nitrogen Vacancies and Carrier-Concentration Control in Rare-Earth Nitrides, *Appl. Phys. Lett.*, 2020, **117**, 222409.
43 S. Chikazumi, Physics of Magnetism John Wiley & Sons, 1964 § 20.2.
44 W. C. Koehler, Magnetic Properties of Rare-Earth Metals and Alloys, *J. Appl. Phys.*, 1965, **36**, 1078–1087.
45 R. M. Bozorth, Magnetic Properties of Compounds and Solid Solutions of Rare-Earth Metals, *J. Appl. Phys.*, 1967, **38**, 1366–1371.

Data for this article are included in the manuscript and the supporting information or are available upon request.